Virtual Coupling of Railway Vehicles: Gap Reference for Merge and Separation, Robust Control, and Position Measurement

Jaegeun Park, *Graduate Student Member, IEEE*, Byung-Hun Lee, *Member, IEEE*, and Yongsoon Eun, *Senior Member, IEEE*

***Abstract*— Virtual coupling, which refers to the operation of railway vehicles that enables the merge and separation of vehicles on the move by controlling the gap between the vehicles without any mechanical coupling, is one of the technologies for increasing the transport capacity and enhancing operational efficiency. This paper proposes a robust gap controller based on sliding mode control with a nonlinear train model with uncertainties. Additionally, a gap reference generation scheme is developed that ensures that the merge and separation of two trains is completed before a given location and respects constraints on acceleration and jerk. The position and velocity measurement errors arising from imperfect knowledge of wheel diameters are also considered, and a new error correction scheme is proposed to reduce the perturbation in the gap control performance. The proposed schemes are validated through simulations.**

***Index Terms*— Sliding model control, virtual coupling, railway vehicles, railway balise.**

I. Introduction

THE transport volume of railways has constantly increased with the development of the goods transportation industry and business travel [1]. Increasing the transport capacity of railways can be achieved by constructing new lines or increasing the capacity of existing lines. Constructing new lines, however, is generally very expensive. Naturally, the railway industry has focused its efforts on increasing the capacity of existing lines and improving railway operational efficiency.

A solution to increase the capacity and enhance the operational efficiency is a system that supports the virtual coupling of trains, where multiple trains merge to form a single train on the move, and a single train also separates into multiple smaller trains as necessary. Specifically, multiple trains merge on the move with the gaps between the trains being much smaller than those allowed by block-based signaling systems (conventional operation is using fixed blocks, where only one train is allowed to exist in a generally hundreds of meters long physical segments of rail called a 'block'), which obviously increases the line capacity. In addition, a train that is longer than the length of the platform at a station may operate by enabling the train to separate near the station into multiple smaller ones such that they stop at multiple parallel platforms. Additionally, at a railway branching point, a longer train may separate and each travel to different destinations, which results in an improved flexibility for better managing the passenger and freight demands. Many operational benefits are expected to be realized once systems that support virtual coupling are in use.

The concept of train virtual coupling was first introduced in [2]–[4] as an innovative operating principle that allows railways to be more attractive than road traffic. Whereas [2] and [3] describe virtual coupling at a conceptual level, [4] additionally discusses train formations and methodological approaches and also demonstrates functionality through simulations at an operational level. Reference [5] discusses the safety aspects for the early concept.

A decade later, the research and development of train virtual coupling has further advanced under the European rail initiative *Shift2Rail*, where the concept and the advantages are reviewed [6]. Here, in addition to the previously discussed advantages in capacity and efficiency, a new aspect for overcoming the disadvantages of mechanical coupling has been discussed, which includes reducing the time to complete the merge/separation of the trains and the compatibility of connecting trains manufactured by different vendors. An effort to modify the train monitoring and control systems that are currently in use to enable virtual coupling has also been made [7], where necessary modifications to the European Rail Traffic Management System/European Train Control System for virtual coupling are proposed. The results are extended in [8], where a virtual coupling control strategy in the automatic train control (ATC) unit is proposed along with numerical simulations of train dynamics to illustrate the performance.

Efforts have also been made to quantitatively demonstrate the benefit of virtually coupled train operation in [9] and [10], where the former reports a seating capacity increase from 15,000 to 23,000 seats per hour for the Japanese 'Shinkansen' high-speed line, and the latter shows up to an approximately 30% reduction of aerodynamic drag, both under the assumption that virtual coupling is enabled.

Manuscript received December 15, 2019; revised June 13, 2020; accepted August 13, 2020. Date of publication September 9, 2020; date of current version February 2, 2022. This work was supported by a Grant from Research and Development Program of the Korea Railroad Research Institute. The Associate Editor for this article was V. Punzo. *(Corresponding author: Yongsoon Eun.)*

Jaegeun Park and Yongsoon Eun are with the Department of Information and Communication Engineering, DGIST, Daegu 42988, South Korea (e-mail: jaegeun2@dgist.ac.kr; yeun@dgist.ac.kr).

Byung-Hun Lee is with the Korea Railroad Research Institute (KRRI), Uiwang 16105, South Korea (e-mail: bhlee85@krri.re.kr).

Digital Object Identifier 10.1109/TITS.2020.3019979

Work on specific gap control algorithms are found in [8], [11] and [12]. Reference [8] proposes a proportional-control-based gap controller in the presence of a known communication delay. A linear quadratic regulator-based gap controller is proposed in [11], which guarantees the string stability of a convoy consisting of multiple trains. The work of [12] proposes a decentralized model-predictive-control-based gap control scheme, which guarantees the gap control performance and stability of a convoy consisting of two trains considering the power, acceleration, and jerk limitation of the train. None of the previous work, however, addresses the uncertainty of the train model. A well known control technique for robustness guarantee is sliding model control (SMC) [13]. For bounded uncertainty, SMC is designed explicitly using the bounds, and the control performance of the resulting system is maintained despite of the disturbance.

The gap controller, in practice, needs to perform in the presence of significant uncertainties: those arise from model parameters and also external disturbances due to rail curve, grade, and rolling resistance. Notice that SMC, in this situation, can provide mathematical guarantees of the performance while other methods in [8], [11], [12] do not.

In this paper, we propose a sliding mode control (SMC) based robust gap controller under model uncertainty and uncertain external disturbances due to rail curve, grade, and rolling resistance. This gap controller guarantees the gap control performance and stability of the resulting closed-loop system under the considered uncertainty. Additionally, an algorithm is developed that computes a gap reference for merge/separation, ensuring the completion of merge/separation before a given location while respecting constraints on the jerk and acceleration of the trains. Finally, the position and velocity measurement errors arising from imperfect knowledge of wheel diameters are considered, and a balise-based position error correction scheme is proposed that reduces gap control perturbations at error correction instances.

Specifically, the uncertainties in the train mass, actuator gain, and external disturbances are treated in the design of the SMC-based gap controller. A bound for the gap-tracking error is guaranteed, and the bound is given with respect to the system parameters and bounds on uncertainties. The gap controller resides in the following train and only affects the movement of the following train. The leading train operates under its own velocity controller and transmits its acceleration command to the gap controller for improved gap control performance. This structure differs from those in [8], [11], and [12].

The algorithm for gap reference generation for merge/separation takes as inputs the position and velocity of the two trains, the location to finish the merge/separation, the gap between the two trains at the point of finishing the merge/separation, the velocity limit of the line, and the jerk and acceleration constraints of the trains. The generated gap reference enables the merge/separation to be completed before a given location while respecting the constraints on the jerk and acceleration of the trains. However, to the best of our knowledge, no studies have considered concrete operating strategies of merge and separation for virtual coupling.

The necessity of the position correction scheme is highlighted as follows: A balise is an electronic beacon placed on the railway as part of an automatic train protection (ATP) system. When passing over a balise, the trains receive the absolute location, based on which the controllers in the trains adjust their positional information. A correction method is necessary because an abrupt adjustment results in perturbation of the control performance. To the best of our knowledge, no studies have addressed the position measurement error or the position error correction in the control for virtual coupling.

Note that virtual coupling, highway vehicle platooning [14]–[16], and cooperative control for multiple trains [17], [18] have many similarities. Vehicle platooning also controls multiple vehicles to maintain a short gap between vehicles to increase highway throughput [14] or reduce fuel consumption [15], [16]. A cooperative control for multiple trains is to coordinate the multiple trains such that they are safely separated and governed steadily under the moving block-based signaling systems by ensuring a safe distance between the trains [17], [18].

The outline of this paper is as follows: In Section 2, the nonlinear train model with uncertainties is given. In Section 3, the system requirements and three modes for virtual coupling are presented. Additionally, we show the gap reference generation scheme for merge/keeping/separation. Finally, the SMC-based gap controller is presented. In Section 4, the existing position error correction scheme is discussed, and the new position error correction scheme is presented. The performance of the SMC-based gap controller and the effectiveness of the proposed position error correction scheme are validated through simulations in Section 5. Finally, conclusions and future work are formulated in Section 6.

II. System Model

The model used in this paper is based on longitudinal train dynamics which includes the train as a point mass, driving/braking systems, and propulsion/grade/curving resistances. The model is given as

$$\begin{aligned} \dot{p}_i(t) &= v_i(t), \\ \dot{v}_i(t) &= \frac{1}{m_i(t)}\left(\alpha_i(t)\mathrm{sat}_F(f_i(t)) - r_i(v_i(t))\right) - w_i(t), \end{aligned} \tag{1}$$

where $i = 1$ denotes the variables for the leading train, and $i = 2$ for the following train. Here, p_i, v_i are the position and the velocity in m and m/s respectively, m_i is the mass in kg, α_i is a uncertain actuator gain, and f_i, $r_i(v_i)$, w_i are the force input in N, disturbance that depends on the velocity in N, and a term that represents the remaining disturbance in $\mathrm{m/s^2}$, respectively.

The function $\mathrm{sat}_F(\cdot)$ denotes the saturation of the force, which is defined as

$$\mathrm{sat}_F(f_i) = \begin{cases} F_{tr}^{\max}(v_i), & \text{if } f_i \geq F_{tr}^{\max}(v_i) \\ -F_{br}^{\max}(v_i), & \text{if } f_i \leq -F_{br}^{\max}(v_i) \\ f_i, & \text{otherwise.} \end{cases} \tag{2}$$

The function $F_{tr}^{\max}(v_i)$ represents the maximum driving force of the traction motor and the function $F_{br}^{\max}(v_i)$ represents the

maximum combined braking force of three types of brakes, i.e, the regenerative brake, the air brake and the disk brake. Reference [19] supports that the two limits are functions of velocity. Note that in this model, the limitation of power is taken into account by the function $F_{tr}^{\max}(v_i)$ and $F_{br}^{\max}(v_i)$ such that $v_i F_{tr}^{\max}(v_i)$ and $v_i F_{br}^{\max}(v_i)$ are both bounded.

The force input f_i represents both driving and braking force, which is the output of an inner loop controller that takes acceleration as an input. Since this inner loop controller dynamics is much faster than velocity control loop, we use

$$f_i(t) = \hat{m}_i(t)\bar{u}_i(t), \tag{3}$$

with $\hat{m}_i$ being the nominal (measured) mass in kg and $\bar{u}_i$ being the conditioned acceleration input in $\mathrm{m/s^2}$. The conditioned acceleration $\bar{u}_i$ is obtained by

$$\bar{u}_i(t) = \mathrm{sat}_J\left(\frac{\mathrm{sat}_A(u_i(t)) - \bar{u}_i(t-\delta)}{\delta}\right)\delta + \bar{u}_i(t-\delta), \tag{4}$$

where u_i is the acceleration input in $\mathrm{m/s^2}$ and δ is the time constant. Equation (4) describes amplitude and rate saturation of the acceleration input using Euler approximation [20] through the functions $\mathrm{sat}_A(\cdot)$ and $\mathrm{sat}_J(\cdot)$ where the two are defined similarly to (2). The subscript A stands for the acceleration and J for the jerk, respectively. The corresponding limits are denoted by $A^{\max}$, $A^{\min}$ and $J^{\max}$, $J^{\min}$. Values of these limits may vary according to the train types. As an instantiation, values of $0.833\ \mathrm{m/s^2}$, $-0.972\ \mathrm{m/s^2}$, $0.8\ \mathrm{m/s^3}$, and $-0.8\ \mathrm{m/s^3}$, respectively, are used in this work for simulations, which are taken from the specifications of Seoul Metro Line 5.

The uncertain actuator gain α_i in (1) captures different characteristics of brakes/motors and also imperfections in the involved inner control loop. The disturbance $r(v_i)$ represents the propulsion resistance, which is defined as the sum of rolling resistance and air resistance [19]. Typically, propulsion resistance is expressed as

$$r_i(v_i) = \mathrm{sgn}(v_i)\left(c_{1,i} + c_{2,i}|v_i| + c_{3,i}v_i^2\right), \tag{5}$$

where $c_{1,i}$ is the term for rolling and bearing resistance, $c_{2,i}$ is a coefficient related to the flange friction, and $c_{3,i}$ is the aerodynamic coefficient. Typically, coefficients $c_{1,i}$, $c_{2,i}$, and $c_{3,i}$ are unknown; however, their nominal values can be obtained empirically. We denote the nominal values by $\hat{c}_{1,i}$, $\hat{c}_{2,i}$, and $\hat{c}_{3,i}$. Finally, the disturbance w_i represents the change in acceleration due to external resistances, such as grade resistance and curving resistance.

We make the following assumptions on the model parameters.

Assumption 1: The train mass measurement error is bounded by a known positive constant M_i, i.e.,

$$|m_i - \hat{m}_i| \le M_i, \tag{6}$$

for $i = 1,\ 2$.

The estimate $\hat{m}_i$ is usually obtained by weight sensors in each car at each stop to accommodate the changes in number of passengers.

Assumption 2: The upper and lower bounds of the parameter α_i are known, i.e.,

$$\alpha_i^{\min} \le \alpha_i \le \alpha_i^{\max}, \tag{7}$$

for $i = 1,\ 2$.

Assumption 3: The three positive constants $C_{1,i}$, $C_{2,i}$, and $C_{3,i}$ are known such that

$$|r_i(v_i) - \hat{r}_i(v_i)| \le R_i(v_i), \tag{8}$$

holds, where $\hat{r}_i(v_i) = \mathrm{sgn}(v_i)\left(\hat{c}_{1,i} + \hat{c}_{2,i}|v_i| + \hat{c}_{3,i}v_i^2\right)$ and $R_i(v_i) = \mathrm{sgn}(v_i)\left(C_{1,i} + C_{2,i}|v_i| + C_{3,i}v_i^2\right)$ for $i = 1,\ 2$.

Assumption 4: A positive constant W_i is known such that

$$|w_i| \le W_i, \tag{9}$$

for $i = 1,\ 2$.

III. Control for Virtual Coupling

A. System Requirements

In this paper, we consider a convoy formed by two virtually coupled trains, as shown in Fig. 1, where d represents the gap between two trains which is defined as

$$d(t) = p_1(t) - l_1 - p_2(t), \tag{10}$$

with l_1 being the length of the leading train. In the convoy, the leading train operates on the operating schedule. Meanwhile, the following train moves, keeping the gap with the leading train equal to the gap reference. For this concept, we assume that the leading train runs with velocity control and that the following train keeps the gap with the leading train using a gap controller, as shown in Fig. 2. Therefore, all trains must equip both a velocity controller and gap controller to select the appropriate controller according to one's role in the convoy.

In most train control systems include two on-board modules: the automatic train protection (ATP) which is responsible for safety and the automatic train operation (ATO) which controls the velocity of train. The SMC based gap controller proposed in this paper is intended to be part of the functions of the ATO. One of the main function of ATP is emergency braking when abnormal operation is detected. The existing ATP may be still used with the virtual coupling enabled ATO (which does not exist yet) to ensure train safety. Emergency braking by ATP is taken into account in the SMC based virtual coupling controller (intended to reside in ATO) in the form of gap reference generation such that the gap is larger than the safety distance.

The following train needs the state information of the leading train, such as its position and velocity, to control the gap with the leading train. The communication channel between the train and the trackside installed in the railway systems can assist the leading train in transmitting its state information to the following train [21]. However, the time delay of the communication channel between the train and the trackside adversely affects the accuracy of the state information of the leading train. In this case, we may use train-to-train communication by means of a Wi-Fi connection or next-generation networks (e.g., 5G) to reduce the communication delay. In this

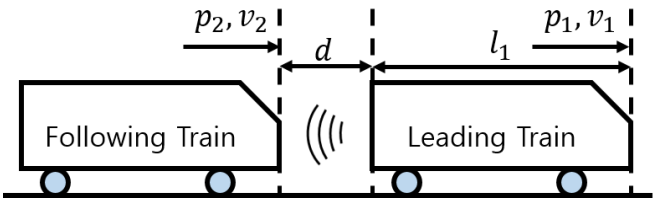

Fig. 1. A convoy with two trains.

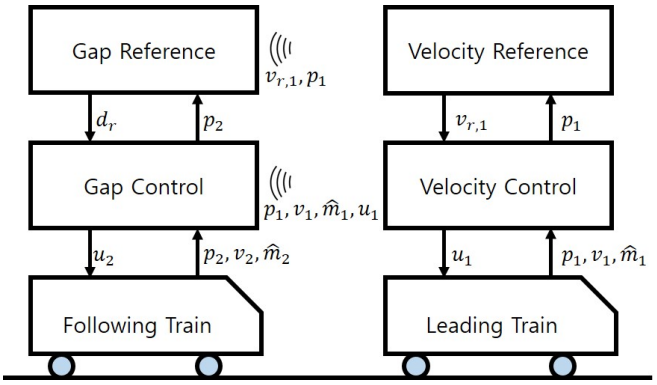

Fig. 2. Control structure for virtual coupling.

paper, communication delay is not explicitly considered due to the following reason. In the virtual coupling control setup, the communication is one way: only the leading train transmits its state to the following train. For small delays, because the leading train always move forward, the gap measurement of the following train in the presence of the delay always yields a smaller value than the actual: at any moment, the leading train already passed its location transmitted to the following train. This is true even in a situation when the leading train is decelerating. Therefore, collision of the two due to communication delay does not take place as long as the gap control performance is maintained. When the delay is significant, a dedicated analysis may be necessary, which is a topic for the future work.

B. Three Modes for Virtual Coupling

An algorithm for virtual coupling has to enable the trains to merge into a convoy, maintain the convoy, and separate the convoy on the move. To implement the virtual coupling algorithm, three modes for virtual coupling, namely, merge, keeping, and separation modes, are defined. The merge mode means decreasing the gap between the two trains to the desired gap between the two trains defined in the keeping mode. The keeping mode is to maintain the convoy formation of the two trains, and the separation mode means increasing the gap between the two trains until they can be recognized as two independent trains.

The section for virtual coupling is assumed to be distinguished in the line, as shown in Fig. 3. The virtual coupling section also consists of merge, keeping, and separation sections. The merge and separation of two trains must be completed in their respective sections.

The procedure for merging two trains is as follows. First, the two trains begin the merge with the following train

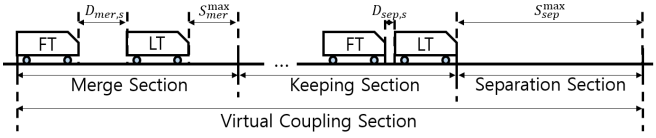

Fig. 3. Virtual coupling section (LT: leading train, FT: following train).

sending the leading train the merge beginning signal when the following train completely enters the merge section, as shown in Fig. 3. Here, we assume that a velocity limit of the merge section $V_{mer}^{\max}$ is constant and that two trains are running at $V_{mer}^{\max}$ at the point of beginning the merge. During the merge, while the following train constantly runs at $V_{mer}^{\max}$, the leading train reduces its velocity to a certain velocity for the merge, denoted as $V_{1,mer}$, to enable the following train to catch up with the leading train. The leading train recovers its velocity to $V_{mer}^{\max}$ at the point of finishing the merge to make the velocities of the leading train and the following train the same. When the two trains are as close as the desired gap between two trains defined in the keeping mode, the merge mode finishes with the following train sending the merge finishing signal to the leading train.

In the keeping mode, the two trains in the convoy formation run keeping the gap between the two trains larger than the safe margin to prevent the collision between the two trains.

The procedure for the separation of the two trains is similar to the procedure for the merge. The two trains begin separating when the leading train sends the separation beginning signal to the following train when the head of the leading train approaches the separation section, as shown in Fig. 3. Similar to the merge, we assume that the velocity limit of the separation section $V_{sep}^{\max}$ is constant and that the two trains are running at $V_{sep}^{\max}$ at the point of finishing the separation. In contrast to the merge, while the leading train runs at $V_{sep}^{\max}$, the following train decreases its velocity to a certain velocity for the separation, denoted as $V_{2,sep}$, to enable the leading train to widen the gap with the following train. The following train recovers its velocity to $V_{sep}^{\max}$ at the point of finishing the separation. When the two trains are far enough apart to be recognized as two independent trains, the separation mode finishes with the following train sending the separation finishing signal to the leading train. Then, the two trains change the mode to the independence mode and independently operate on each schedule.

C. Gap Reference Generation

We propose a gap reference generation scheme for virtual coupling. The goal of gap reference generation for the merge/separation is to ensure the completion of merge/separation before a given location while respecting the constraints on the jerk and acceleration of the trains. The gap reference, which is denoted as d_r, is represented such that

$$d_r(t) = \begin{cases} d_{r,mer}(t), & \text{if } t \in [t_{mer},\ t_{keep}) \\ d_{r,keep}(t) & \text{if } t \in [t_{keep},\ t_{sep}) \\ d_{r,sep}(t), & \text{if } t \in [t_{sep},\ t_{ind}), \end{cases} \tag{11}$$

where $d_{r,mer}$, $d_{r,keep}$, and $d_{r,sep}$ are the gap references of the merge, keeping, and separation modes, respectively. Additionally, t_{mer}, t_{keep}, t_{sep}, and t_{ind} are the points of beginning the merge, keeping, separation, and independence modes, respectively.

At the point of beginning the merge of two trains, the gap between the two trains and the travel distance of the two trains are determined such that

$$\begin{aligned} D_{mer,b} &= p_1(t_{mer}) - l_1 - p_2(t_{mer}), \\ S_{1,mer} &= L_{mer,e} - p_1(t_{mer}), \\ S_{2,mer} &= S_{1,mer} + D_{mer,b} - D_{mer,f}, \end{aligned} \tag{12}$$

where $D_{mer,b}$ denotes the gap between the two trains at the point of beginning the merge, $S_{1,mer}$ denotes the travel distance of the leading train during the merge, $L_{mer,e}$ denotes the end location of the merge section, and $S_{2,mer}$ denotes the travel distance of the preceding train. Additionally, the gap between the two trains at the point of finishing the merge is denoted as $D_{mer,f}$, which is obtained by

$$D_{mer,f} = \rho_1 v_{1,r}(t_{mer} + T_{mer}) + \rho_2, \tag{13}$$

where the positive constants ρ_1 and ρ_2 denote design parameters of the gap reference for the keeping mode. The travel time of the merge is denoted as T_{mer}, i.e., $v_1(t_{mer} + T_{mer})$ denotes the velocity of the leading train at the point of finishing the merge. As described in Subsection III-C, the velocity of the leading train is recovered to the velocity limit of the merge section at the point of finishing the merge, i.e., $v_1(t_{mer} + T_{mer}) = V_{mer}^{\max}$.

In the merge mode, the leading train reduces its velocity from $V_{mer}^{\max}$ to $V_{1,mer}$. The velocity $V_{1,mer}$ is obtained by

$$V_{1,mer} = \frac{-B + \sqrt{B^2 - 4AC}}{2A}, \tag{14}$$

where A, B, C, and D are as follows:

$$\begin{aligned} A &= -\frac{1}{2A^{\min}} + \frac{1}{2A^{\max}}, \\ B &= T_{mer} + \left(\frac{v_1(t_{mer})}{A^{\min}} - \frac{|A^{\min}|}{2|J^{\min}|}\right) \\ &\quad + \left(\frac{-v_1(t_{mer} + T_{mer})}{A^{\max}} - \frac{|A^{\max}|}{2|J^{\min}|}\right), \\ C &= \left(\frac{v_1(t_{mer})}{A^{\min}} - \frac{|A^{\min}|}{2|J^{\min}|}\right) \\ &\quad + \left(\frac{-v_1(t_{mer} + T_{mer})}{A^{\max}} - \frac{|A^{\max}|}{2|J^{\min}|}\right) - S_{1,mer}. \end{aligned} \tag{15}$$

The velocity of the leading train at the point of beginning the merge is denoted as $v_1(t_{mer})$, which is assumed to be the velocity limit of the merge $V_{mer}^{\max}$, i.e., $v_1(t_{mer}) = V_{mer}^{\max}$. The travel time for the merge is denoted as T_{mer}, which is obtained by

$$T_{mer} = \frac{S_{2,mer}}{V_{mer}^{\max}}, \tag{16}$$

under the assumption that the following train constantly runs at the velocity limit of the merge section $V_{mer}^{\max}$ during the merge. Note that if $4AC$ in (14) and (15) is positive, then $V_{1,mer}$ becomes negative, and it means that the merge of two trains is impossible. From this, we can derive the maximum gap between two trains at the point of beginning the merge enabling the merge $D_{mer,b}^{\max}$ such that

$$\begin{aligned} D_{mer,b}^{\max} = L_{mer,e} - L_{mer,s} - l_1 - l_2 - \left(\frac{V_{mer}^{\max}}{A^{\min}}\right. \\ \left. - \frac{|A^{\min}|}{2|J^{\min}|}\right) + \left(\frac{-V_{mer}^{\max}}{A^{\max}} - \frac{|A^{\max}|}{2|J^{\min}|}\right), \end{aligned} \tag{17}$$

where $L_{mer,s}$ denotes the start location of the merge section.

The velocity of the leading train during the merge $v_{1,mer}$ is represented as

$$v_{1,mer}(t) = \begin{cases} v_1(t_{mer}) + \dfrac{J^{\min}}{2}(t - \min\{I_1\})^2, & \text{if } t \in I_1, \\ v_1(t_{mer}) + \dfrac{J^{\min}}{2}(T_1)^2 + A^{\min}(t - \min\{I_2\}), & \text{if } t \in I_2, \\ v_1(t_{mer}) + \dfrac{J^{\min}}{2}(T_1)^2 + A^{\min}(T_2) & \\ \quad + A^{\min}(t - \min\{I_2\}) + \dfrac{J^{\max}}{2}(t - \min\{I_3\})^2, & \text{if } t \in I_3, \\ V_{1,mer}, & \text{if } t \in I_4 \\ V_{1,mer} + \dfrac{J^{\max}}{2}(t - \min\{I_5\})^2, & \text{if } t \in I_5, \\ V_{1,mer} + \dfrac{J^{\max}}{2}(T_5)^2 + A^{\max}(t - \min\{I_6\}), & \text{if } t \in I_6, \\ V_{1,mer} + \dfrac{J^{\max}}{2}(T_5)^2 + A^{\max}(T_6) & \\ \quad + A^{\max}(t - \min\{I_6\}) + \dfrac{J^{\min}}{2}(t - \min\{I_7\})^2, & \text{if } t \in I_7, \end{cases} \tag{18}$$

where $T_1 = \left|\frac{A^{\min}}{J^{\min}}\right|$, $T_2 = \frac{V_{1,mer} - v_1(t_{mer})}{A^{\min}} - \left|\frac{A^{\min}}{2J^{\min}}\right| - \left|\frac{A^{\min}}{2J^{\max}}\right|$, $T_4 = T_{mer} - (T_1 + T_2 + T_3 + T_5 + T_6 + T_7)$, $T_5 = \left|\frac{A^{\max}}{J^{\max}}\right|$, $T_6 = \frac{V_{mer}^{\max} - V_{1,mer}}{A^{\max}} - \left|\frac{A^{\max}}{2J^{\max}}\right| - \left|\frac{A^{\max}}{2J^{\min}}\right|$, and $T_7 = \left|\frac{A^{\max}}{J^{\min}}\right|$. The set $I_1 = \{t \mid t \in \mathbb{R},\ t_{mer} \le t < t_{mer} + T_1\}$, where $\mathbb{R}$ denotes the set of real numbers. Similarly, the set $I_i = \{t \mid t \in \mathbb{R},\ \sup\{I_{i-1}\} \le t < \sup\{I_{i-1}\} + T_i\}$ for $i = 2,\ 3,\ \ldots,\ 7$.

Because the following train constantly runs at $V_{mer}^{\max}$ during the merge, the velocity of the following train during the merge $v_{2,mer}$ is such that

$$v_{2,mer}(t) = V_{mer}^{\max}. \tag{19}$$

Finally, the gap reference $d_{r,mer}$ for the merge is obtained by

$$d_{r,mer}(t) = D_{mer,b} + \int_{t_{mer}}^{t} \left(v_{1,mer}(\tau) - v_{2,mer}(\tau)\right)\, d\tau. \tag{20}$$

Fig. 4 shows an example of the velocity reference of two trains and the gap reference for the merge of two trains.

The gap reference for the keeping mode $d_{r,keep}$ is obtained by

$$d_{r,keep}(t) = \rho_1 v_{1,r}(t) + \rho_2, \tag{21}$$

where $v_{1,r}$ denotes the velocity reference of the leading train that is transmitted from the leading train, the positive constant ρ_1 is the headway time between the two trains, and the positive

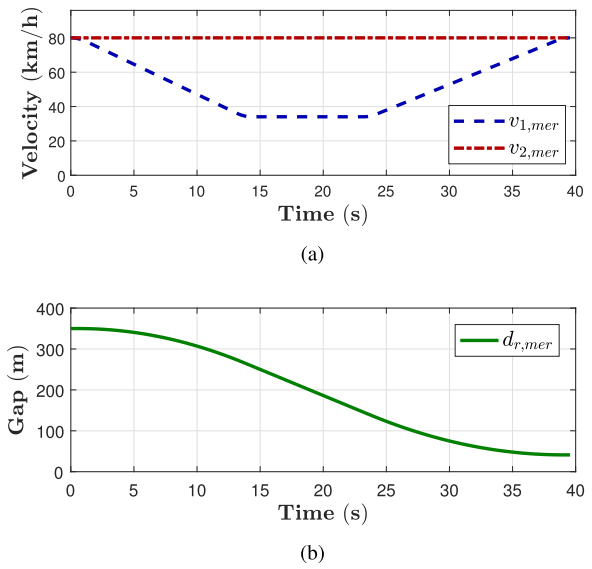

Fig. 4. An example of (a) the velocity of two trains and (b) the gap reference for the merge.

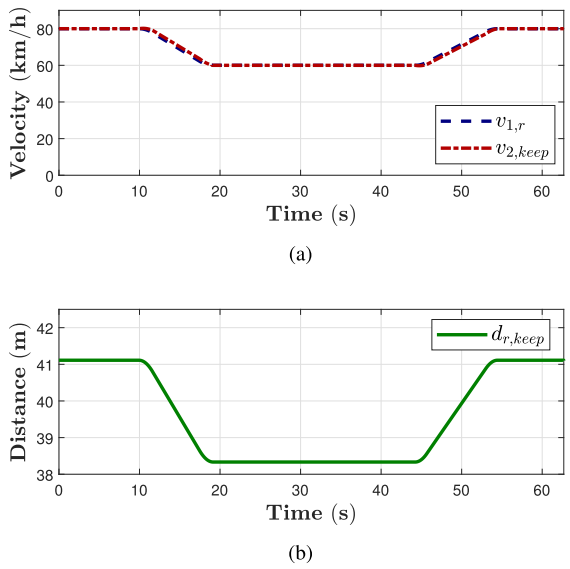

Fig. 5. An example of (a) the velocity reference of the leading train, the velocity of the following train and (b) the gap reference for the keeping.

constant ρ_2 is the gap between the two trains at standstill. The constants ρ_1 and ρ_2 have to be chosen such that $d_{r,keep}$ is larger than the safe margin d_{safe} in order to enable emergency braking while keeping virtual coupling. The safe margin d_{safe} is obtained by

$$d_{safe}(t) = \frac{(v_2(t)+\Delta V^{\max})^2}{2EB_2^{\min}} - \frac{(v_1(t)-\Delta V^{\max})^2}{2EB_1^{\max}} + 2\Delta P^{\max}. \tag{22}$$

In the safe margin formulation, uncertainties of emergency braking deceleration, position measurement, and velocity measurement are taken into account. The uncertain emergency braking deceleration is defined as $EB_i := \left\{x \in \mathbb{R} \;\; EB_i^{\min} \leq x \leq EB_i^{\max}\right\}$, where $EB_i^{\min}$ and $EB_i^{\max}$ are positive constants. Also, the position measurement error $\Delta p_i(t)$ and the velocity measurement error $\Delta v_i(t)$ are assumed as $|\Delta p_i(t)| \leq \Delta P^{\max}$ and $|\Delta v_i(t)| \leq \Delta V^{\max}$, where $\Delta P^{\max}$ and $\Delta V^{\max}$ are positive constants.

If the following train runs while keeping the gap with the leading train as much as $d_{r,keep}$, the acceleration of the following train $a_{2,keep}$ is such that

$$a_{2,keep}(t) = \dot{v}_{1,r}(t) - \rho_1 \ddot{v}_{1,r}(t). \tag{23}$$

Note that because the following train has the saturation of acceleration, $v_{1,r}$ and ρ_1 in (23) have to be selected such that $a_{2,keep}$ is within the saturation of acceleration of the following train. Fig. 5 shows an example of the velocity reference of the leading train $v_{1,r}$, the velocity of the following train $v_{2,keep}$ and the gap reference for the keeping mode.

The gap reference for the separation $d_{r,sep}$ can be obtained by changing the roles of the leading train and the following train in the gap reference generation for the merge. Fig. 6 shows an example of the velocity reference of two trains and the gap reference for the separation of two trains.

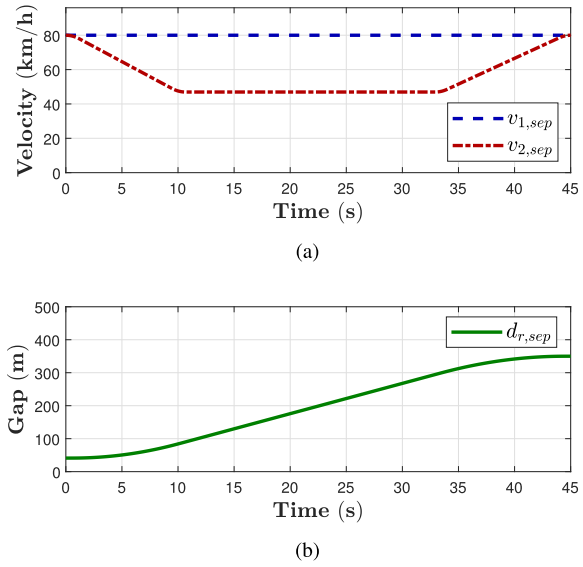

Fig. 6. An example of (a) the velocity of two trains and (b) the gap reference for the separation mode.

D. SMC-Based gap Controller Design

In this paper, the SMC-based gap controller is proposed as the robust gap controller under model uncertainty and uncertain external disturbances. In the design of the gap controller, we consider the train model except for saturation as follows:

$$\begin{aligned} \dot{p}_i &= v_i, \\ \dot{v}_i &= \frac{1}{m_i}\left(\alpha_i f_i - r_i(v_i)\right) - w_i, \\ f_i &= \hat{m}_i u_i. \end{aligned} \tag{24}$$

The model of the gap between two trains d in (10) is derived with (24) such that

$$\begin{aligned} \dot{d} &= v_1 - v_2, \\ \ddot{d} &= g(v_1, v_2, \hat{m}_1, u_1) - h(\hat{m}_2)u_2, \end{aligned} \tag{25}$$

where the functions $g(v_1, v_2, \hat{m}_1, u_1)$ and $h(\hat{m}_2)$ are given by

$$g(v_1, v_2, \hat{m}_1, u_1) = \frac{\hat{m}_1}{m_1}\alpha_1 u_1 - \left(\frac{1}{m_1}r_1(v_1) - \frac{1}{m_2}r_2(v_2)\right) - (w_1 - w_2),$$
$$h(\hat{m}_2) = \frac{\hat{m}_2}{m_2}\alpha_2. \tag{26}$$

Under Assumptions 1-4, the inequalities of $g(v_1, v_2, \hat{m}_1, u_1)$ and $h(\hat{m}_2)$ are derived such that

$$|g(v_1, v_2, \hat{m}_1, u_1) - \hat{g}(v_1, v_2, \hat{m}_1, \hat{m}_2, u_1)| \le G(v_1, v_2, \hat{m}_1, \hat{m}_2, u_1), \tag{27}$$
$$\beta^{-1}(\hat{m}_2) \le \frac{\hat{h}(\hat{m}_2)}{h(\hat{m}_2)} \le \beta(\hat{m}_2), \tag{28}$$

where $\hat{g}(v_1, v_2, \hat{m}_1, \hat{m}_2, u_1)$ and $\hat{h}(\hat{m}_2)$ denote the nominal $g(v_1, v_2, \hat{m}_1, u_1)$ and the nominal $h(\hat{m}_2)$, respectively, which are obtained by

$$\hat{g}(v_1, v_2, \hat{m}_1, \hat{m}_2, u_1) = u_1 - \frac{1}{\hat{m}_1}\hat{r}_1(v_1) + \frac{1}{\hat{m}_2}\hat{r}_2(v_2), \tag{29}$$
$$\hat{h}(\hat{m}_2) = \sqrt{h^{\max}(\hat{m}_2)h^{\min}(\hat{m}_2)}. \tag{30}$$

In (30), $h^{\max}(\hat{m}_2)$ and $h^{\min}(\hat{m}_2)$ are the maximum and the minimum of $h(\hat{m}_2)$, respectively, which are given by

$$h^{\max}(\hat{m}_2) = \frac{\hat{m}_2\alpha_2^{\max}}{\hat{m}_2 - M_2}, \quad h^{\min}(\hat{m}_2) = \frac{\hat{m}_2\alpha_2^{\min}}{\hat{m}_2 + M_2}. \tag{31}$$

The bounds $G(v_1, v_2, \hat{m}_1, \hat{m}_2, u_1)$ and $\beta(\hat{m}_2)$ are obtained by

$$G(v_1, v_2, \hat{m}_1, \hat{m}_2, u_1) = \left|\left(\frac{\hat{m}_1\alpha_1^{\max}}{\hat{m}_1 - M_1} - 1\right)u_1\right| + \frac{1}{\hat{m}_1 - M_1}R_1(v_1) + \frac{M_1}{(\hat{m}_1 - M_1)\hat{m}_1}\hat{r}_1(v_1) + \frac{1}{\hat{m}_2 - M_2}R_2(v_2) + \frac{M_2}{(\hat{m}_2 - M_2)\hat{m}_2}\hat{r}_2(v_2) + W_1 + W_2, \tag{32}$$
$$\beta(\hat{m}_2) = \sqrt{\frac{h^{\max}(\hat{m}_2)}{h^{\min}(\hat{m}_2)}}, \tag{33}$$

The control input u_2 of the following train in the system of (25) is given by

$$u_2 = -\hat{h}^{-1}(\hat{m}_2)\left(\hat{u}_2(v_2) - \bar{k}\,\mathrm{sat}\left(\frac{s}{\phi}\right)\right), \tag{34}$$

where $\mathrm{sat}\left(\frac{s}{\phi}\right)$ is defined as

$$\mathrm{sat}\left(\frac{s}{\phi}\right) = \begin{cases} 1, & \text{if } s \ge \phi, \\ -1, & \text{if } s \le -\phi, \\ \dfrac{s}{\phi}, & \text{otherwise.} \end{cases} \tag{35}$$

Additionally, s of (34) is defined as

$$s = \dot{\tilde{d}} + \lambda\tilde{d}, \tag{36}$$

where the positive constant λ is the design parameter, and the gap-tracking error $\tilde{d}$ is defined as

$$\tilde{d} = d - d_r. \tag{37}$$

In (34), $\hat{u}_2(v_2)$ is given by

$$\hat{u}_2(v_2) = -\hat{g}(v_1, v_2, \hat{m}_1, \hat{m}_2, u_1) + \ddot{d}_r - \lambda\dot{\tilde{d}}, \tag{38}$$

and $\bar{k}$ is written as

$$\bar{k} = \begin{cases} k(v_2) - \dfrac{\dot{\phi}}{\beta(\hat{m}_2)}, & \text{if } k\left(v_1 - \dot{d}_r\right) \ge \dfrac{\lambda\phi}{\beta(\hat{m}_2)}, \\ k(v_2) - \beta(\hat{m}_2)\dot{\phi}, & \text{otherwise,} \end{cases} \tag{39}$$

where

$$k(v_2) = \beta(\hat{m}_2)(G(v_1, v_2, \hat{m}_1, \hat{m}_2, u_1) + \eta) + (\beta(\hat{m}_2) - 1)|\hat{u}_2(v_2)|. \tag{40}$$

Here, the positive constant η is the design parameter. The dynamics of ϕ is represented as

$$\dot{\phi} = \begin{cases} -\lambda\phi + \beta(\hat{m}_2)k\left(v_1 - \dot{d}_r\right), & \text{if } k\left(v_1 - \dot{d}_r\right) \ge \dfrac{\lambda\phi}{\beta(\hat{m}_2)}, \\ -\dfrac{\lambda\phi}{(\beta(\hat{m}_2))^2} + \dfrac{k\left(v_1 - \dot{d}_r\right)}{\beta(\hat{m}_2)}, & \text{otherwise,} \end{cases} \tag{41}$$

where the initial condition of ϕ is given by

$$\phi(0) = \frac{\beta(\hat{m}_2(0))k\left(v_1(0) - \dot{d}_r(0)\right)}{\lambda}. \tag{42}$$

The following theorem shows that the control input u_2 obtained by SMC makes the gap-tracking error $\tilde{d}$ have bounds.

Theorem 1: Let Assumptions 1-4 hold. Consider the closed-loop system of (25), (26) and (27)-(42). Then, the following inequality holds:

$$|\tilde{d}| \le \frac{\beta(\hat{m}_2)k(v_1 - \dot{d}_r)}{\lambda^2}. \tag{43}$$

Proof: See Appendix. ∎

Thus, Theorem 1 guarantees that the gap-tracking error $|\tilde{d}|$ is bounded. Note that the bound is a function of the acceleration of two trains, which means that the guaranteed gap-tracking error bound is proportional to the size of the acceleration of two trains.

IV. Position Error Correction

Starting in this section, we consider the velocity and position measurement errors of the train. In railway control systems, the velocity of the train is measured by a tachometer, which leads to velocity measurement error due to imperfect knowledge of wheel diameters. The position is also measured by integrating the velocity measurement, which makes the position measurement error infinitely increase. For this reason, railway control systems correct the position measurement error by changing the position measurement into the absolute location received from the balise when the train passes over the balise. However, the position measurement has discontinuous points at the error correction instances, which leads to gap control perturbations. Therefore, we propose a new position error correction scheme to reduce the gap control perturbations.

A. The Existing Position Error Correction Scheme

The velocity measurement of the i-th train $v_{i,m}$ is defined as

$$v_{i,m}(t) = v_i(t) + \Delta v_i(t), \tag{44}$$

where v_i is the actual velocity and Δv_i is the velocity measurement error. We make the following assumption on the velocity measurement arising from imperfect knowledge of the wheel diameters.

Assumption 5: The measurement error of velocity Δv_i is the sum of proportional value to actual velocity v_i and zero-mean Gaussian noise and is represented by

$$\Delta v_i(t) = \mu_i v_i(t) + \xi_i(t), \tag{45}$$

where the constant μ_i is unknown and ξ_i is zero-mean Gaussian noise, i.e., $E\{\xi_i\} = 0$.

The position measurement obtained by integrating the velocity measurement is defined as

$$p_{i,m}(t) = p_i(t) + \Delta p_i(t), \tag{46}$$

where p_i and Δp_i denote the actual position and the position measurement error, respectively, which are written as

$$p_i(t) = \int_0^t v_i(\tau) d\tau, \quad \Delta p_i(t) = \int_0^t \Delta v_i(\tau) d\tau, \tag{47}$$

and under Assumption 5, the expectation of Δp_i is represented as

$$E\{\Delta p_i(t)\} = \mu_i \int_0^t v_i(\tau) d\tau. \tag{48}$$

Note that the size of the position measurement error increases infinitely for $t \to \infty$. Thus, in railway control systems, the position measurement is corrected by substituting absolute location information received from the balise, i.e., the corrected position measurement $\bar{p}_{i,m}$ is written as

$$\bar{p}_{i,m}(t) = p_i(t) + \Delta \bar{p}_i(t), \tag{49}$$

where $\Delta \bar{p}_i$ denotes the corrected position measurement error, which is given by

$$\Delta \bar{p}_i(t) = \int_{t_{j,i}}^t \Delta v_i(\tau) d\tau, \quad \text{for } t_{j,i} \le t < t_{j+1,i}, \quad j = 0, 1, 2, \ldots \tag{50}$$

where $t_{j,i}$ denotes the point at which the i-th train passes the j-th balise, and $t_{0,i}$ means the point at which the i-th train begins, i.e., $t_{0,i} = 0$. The expectation of the corrected position measurement error is also obtained by

$$E\{\Delta \bar{p}_i(t)\} = \int_{t_{j,i}}^t \mu_i v_i(\tau) d\tau, \quad \text{for } t_{j,i} \le t < t_{j+1,i}, \quad j = 0, 1, 2, \ldots \tag{51}$$

Note that the expectation of the corrected position measurement error $E\{\Delta \bar{p}_i(t)\}$ when the train passes over the balise is zero.

Under the assumption that balises are installed at regular intervals, which are denoted as D_b, the size of the expectation of the corrected position measurement error $|E\{\Delta \bar{p}_i\}|$ satisfies the inequality such that

$$|E\{\Delta \bar{p}_i(t)\}| < |\mu_i D_b|, \tag{52}$$

From (51), the differentiation of the expectation of the corrected position measurement error is induced such that

$$\begin{aligned} &\frac{dE\{\Delta \bar{p}_i(t)\}}{dt} \\ &= \lim_{\delta \to 0} \frac{E\{\Delta \bar{p}_i(t)\} - E\{\Delta \bar{p}_i(t-\delta)\}}{t - (t-\delta)}, \\ &= \begin{cases} \lim_{\delta \to 0} \dfrac{-\mu_i (D_b - (p_i(t) - p_i(t-\delta))}{\delta}, & \text{if } t = t_{j,i}, \\ \mu_i v_i(t), & \text{otherwise}, \end{cases} \end{aligned} \tag{53}$$

for $j = 0, 1, 2, \ldots$. Note that the corrected position measurement error has discontinuous points when the train passes over the balise in (53), and it also means that the gap measurement in the gap controller has discontinuous points, which results in perturbations in the gap control.

B. The Proposed Position Error Correction Scheme

In this section, we introduce the new position error correction scheme to reduce perturbations in the gap control. The concept of the proposed position error correction scheme is to gradually reduce the position measurement error obtained when the train passes over the balise to zero in the next balise. For this concept, the position measurement error corrected by the proposed error correction scheme can be expressed as

$$\begin{aligned} &\Delta \bar{p}_i(t) \\ &= \Delta \bar{p}_i(t_{j,i}) \left(1 - \frac{\int_{t_{j,i}}^t v_{i,m}(\tau)\, d\tau}{D_b}\right) + \int_{t_{j,i}}^t \Delta v_i(\tau)\, d\tau, \\ &\qquad \text{for } t_{j,i} \le t < t_{j+1,i}, \quad j = 0, 1, 2, \ldots . \end{aligned} \tag{54}$$

The expectation of the position measurement error corrected by the proposed error correction scheme is also written as

$$\begin{aligned} E\{\Delta \bar{p}_i(t)\} &= E\{\Delta \bar{p}_i(t_{j,i})\} \\ &\quad + \left(\mu_i - \frac{\mu_i + 1}{D_b} E\{\Delta \bar{p}_i(t_{j,i})\}\right) \int_{t_{j,i}}^t v_i(\tau)\, d\tau, \\ &\qquad \text{for } t_{j,i} \le t < t_{j+1,i}, \quad j = 0, 1, 2, \ldots . \end{aligned} \tag{55}$$

The expectation of the position measurement error, which is corrected by the proposed scheme when the train passes over the balise, is given by

$$E\{\Delta \bar{p}_i(t_{j+1,i})\} = -\mu_i E\{\Delta \bar{p}_i(t_{j,i})\} + \mu_i D_b \quad \text{for } t_{j,i} \le t < t_{j+1,i}, \quad j = 0, 1, 2, \ldots . \tag{56}$$

If j goes to infinity, i.e., the train passes sufficiently many balises, then the expectation of the position measurement error is obtained by

$$\lim_{j \to \infty} E\{\Delta \bar{p}_i(t_{j,i})\} = \begin{cases} \dfrac{\mu_i D_b}{\mu_i + 1}, & \text{if} |\mu_i| < 1, \\ \infty, & \text{otherwise}. \end{cases} \tag{57}$$

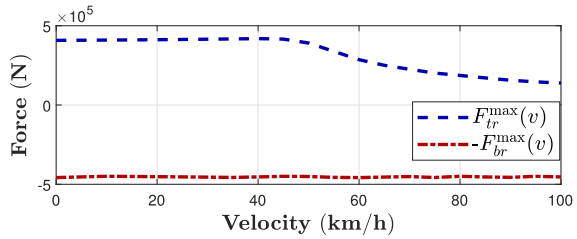

Fig. 7. The saturation of force in the simulation.

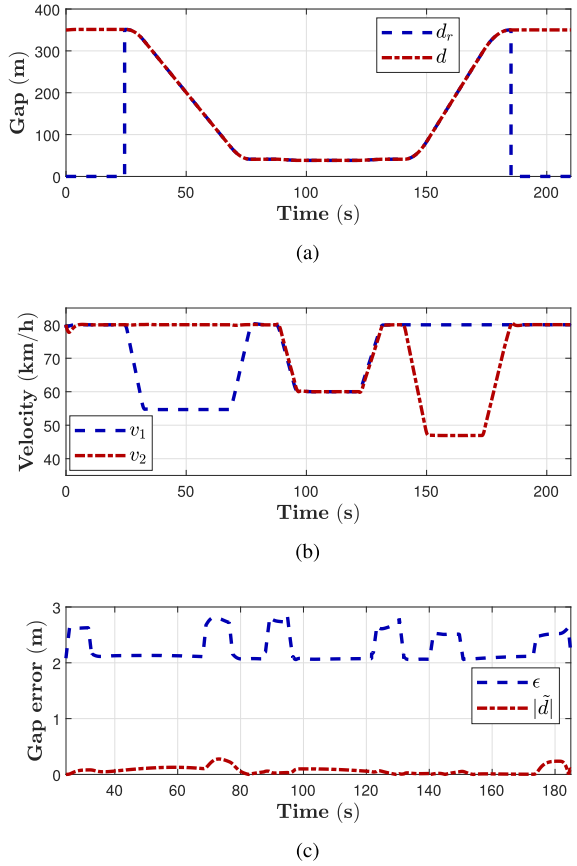

Fig. 8. The simulation result for validating the performance for the SMC-based gap controller ((a) d_r: the gap reference, d: the gap between two trains; (b) the velocity of two trains; (c) ϵ: the upper bound of the gap-tracking error, $|\tilde{d}|$: the size of the gap-tracking error).

From (55) and (57), we can induce the equation such that

$$\lim_{t\to\infty} E\{\Delta \bar{p}_i(t)\} = \begin{cases} \dfrac{\mu_i D_b}{\mu_i + 1}, & \text{if} |\mu_i| < 1, \\ \infty, & \text{otherwise.} \end{cases} \tag{58}$$

Note that if $|\mu_i|$ is smaller than 1, then the expectation of the position measurement error corrected by the proposed scheme converges, but if it is not, it diverges. Therefore, for utilizing the proposed position error correction scheme, the velocity sensor of trains, such as the tachometer, has to be designed that the size of the constant μ_i is smaller than 1. Moreover, note that if $|\mu_i|$ is smaller than 1, the differentiation of the expectation of the position measurement error corrected by the proposed scheme also converges to zero, i.e., this position error correction scheme exactly removes perturbations in gap control.

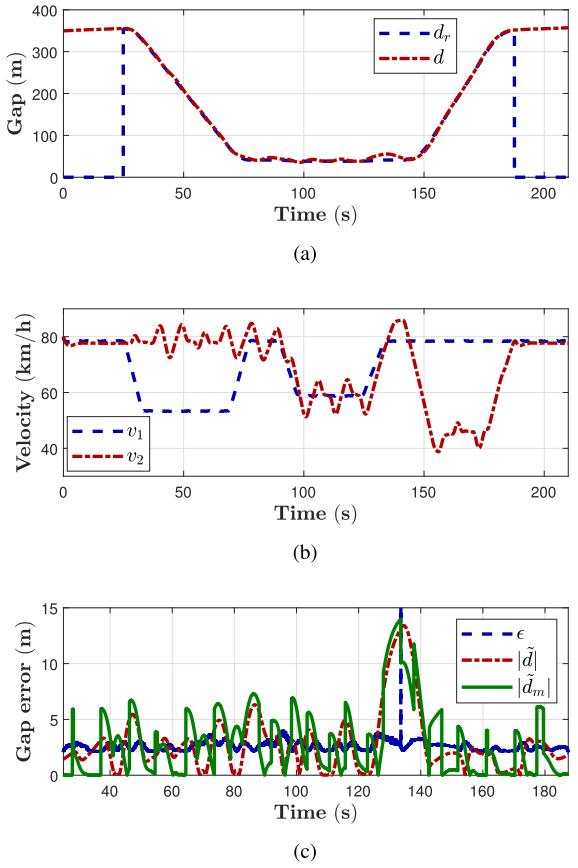

Fig. 9. The simulation result for verifying the effect of the existing position error correction scheme on gap controller ((a) d_r: the gap reference, d: the gap between two trains; (b) the velocity of two trains; (c) ϵ: the upper bound of the gap-tracking error, $|\tilde{d}|$: the size of the gap-tracking error, $\tilde{d}_m$: the size of $d_m - d_r$).

V. Simulations

In this section, we validate the performance of the SMC-based gap controller in a scenario in which two trains consecutively conduct the merge, the keeping, and the separation, and we evaluate the effectiveness of the proposed position error correction scheme with the same scenario. In the simulation, the train model of (1) is used, and the two trains have the same saturation of force, acceleration and jerk. All the parameters of the train model and the coefficients of the nominal propulsion resistance are taken from the Train Maintenance Guideline for Seoul Metro Line 5. The maximum traction force $F_{tr}^{\max}(v_i)$ and the maximum braking force $F_{br}^{\max}(v_i)$ of the force saturation are chosen as shown in Fig. 7, and the maximum and the minimum value of the acceleration and jerk are chosen as $A^{\max} = 0.833$ m/s^2, $A^{\min} = -0.972$ m/s^2, $J^{\max} = 0.8$ m/s^3, and $J^{\min} = -0.8$ m/s^3. The nominal mass and coefficients of the nominal propulsion resistance are chosen as $\hat{m}_1 = \hat{m}_2 = 262800$ kg, $\hat{c}_{1,1} = \hat{c}_{1,2} = 4808.3$, $\hat{c}_{2,1} = \hat{c}_{2,2} = 92.46$, and $\hat{c}_{3,1} = \hat{c}_{3,2} = 1.92$. The parameters in Assumptions 1-4 are chosen as $M_1 = 0.1\hat{m}_1$, $M_2 = 0.1\hat{m}_2$, $\alpha_1^{\max} = \alpha_2^{\max} = 1.2$, $\alpha_1^{\min} = \alpha_2^{\min} = 0.8$, $C_{1,1} = 0.2\hat{c}_{1,1}$, $C_{1,2} = 0.2\hat{c}_{1,2}$, $C_{2,1} = 0.2\hat{c}_{1,2}$, $C_{2,2} = 0.2\hat{c}_{2,2}$, $C_{3,1} = 0.2\hat{c}_{3,1}$, $C_{3,2} = 0.2\hat{c}_{3,3}$, and $W_1 = W_2 = 0.05$ m/s^2. Uncertainty variables are also selected such that $m_1 = 268056$ kg, $m_2 = 252288$ kg, $c_{1,1} = 4615.968$,

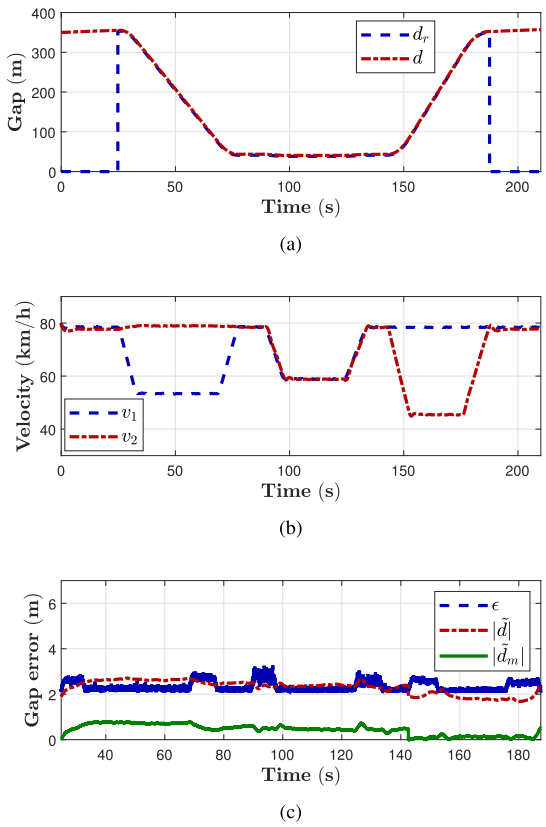

Fig. 10. The simulation result for verifying the effect of the proposed position error correction scheme on gap controller ((a) d_r: the gap reference, d: the gap between two trains; (b) the velocity of two trains; (c) ϵ: the upper bound of the gap-tracking error, $|\tilde{d}|$: the size of the gap-tracking error, $\tilde{d}_m$: the size of $d_m - d_r$).

$c_{1,2} = 4856.383$, $c_{2,1} = 81.365$, $c_{2,2} = 93.3846$, $c_{3,1} = 1.824$, $c_{3,2} = 2.208$, $w_1 = 0.02$ m/s^2, and $w_2 = -0.01$ m/s^2.

In all the simulations, the design parameters of the SMC-based gap controller are the same, which are chosen as $\eta = 1$ and $\lambda = 1$. Furthermore, the design parameters of the gap reference of the keeping mode are chosen as $\rho_1 = 0.5$ and $\rho_2 = 30$.

A. Performance of the SMC-Based gap Controller

We conduct the simulation in a scenario in which two trains consecutively conduct the merge, the keeping, and the separation to validate the feasibility of virtual coupling and the performance of the SMC-based gap controller. The velocity limit of all the lines is 80 km/h. As shown in Fig. 8(a), the merge, keeping, and separation started at 25.9, 53.2, and 204 seconds, respectively. The gap reference d_r during the remaining time is zero, which means that the two trains run independently with each velocity control. As shown in Fig. 8(b), in the merge mode, the leading train reduces its velocity to allow the following train to catch up, and the following train runs at the velocity limit of the line. In the keeping mode, the following train follows the leading train at the time interval of the headway time ρ_1 of (21). In the separation mode, the following train reduces its velocity to allow the leading train to widen the gap between them, and the leading train runs at the velocity limit of the line. Fig. 8(c) shows that the size of the gap-tracking error $|\tilde{d}|$ is smaller than ϵ, which denotes the upper bound in (43), i.e., Theorem 1 is validated in this simulation. We can also confirm that the ϵ increases when the velocity of the leading train or the following train is changed.

B. Effectiveness of the Proposed Position Error Correction Scheme

In the simulation for Fig. 9 and Fig. 10, we apply the measurement errors of velocity and position to the simulation for Fig. 8 to verify the effectiveness of the proposed position error correction scheme, where $\mu_1 = 0.02$, $\mu_2 = 0.03$ in (45). Moreover, the gap between balises is chosen as $D_b = 200$ m. Fig. 9 and Fig. 10 show the simulation results when applying the existing position error correction scheme and the proposed position error correction scheme, respectively. Through these results, we can compare the effects of the two position error correction schemes on the gap controller. First, Fig. 9 shows that the velocity of the following train v_2 oscillates and $|\tilde{d}_m|$ obtained by $|d_m - d_r|$ is almost larger than ϵ. On the other hand, in Fig. 10, the oscillation in the velocity of the following train v_2 disappears and $|\tilde{d}_m|$ is smaller than ϵ, i.e., the gap control perturbations disappear.

VI. Conclusion and Future Work

This paper has proposed a robust gap controller for virtual coupling. For the robust gap controller design, the nonlinear train model with uncertainties is given, and bounds on uncertainties of actuator gain, mass measurement, propulsion resistance, and external disturbances, which include curving and grade resistance, are assumed. The gap reference generation scheme is developed to ensure that the merge/separation is completed before a given location while respecting constraints on the jerk and acceleration of the trains. The proposed robust gap controller is based on sliding mode control. The mathematical analysis for the robustness of the SMC-based gap controller is conducted. A new position error correction scheme based on balises is proposed to reduce gap control perturbations. The proposed position error correction scheme makes the position measurement error diminish over time in a smooth manner, which removes gap control perturbations. Future work includes extending the SMC-based control scheme to virtually couple three or more trains.

Appendix
Proof of Theorem 1

Consider $|s| > \phi$. Define the function V to be

$$V = \frac{1}{2}s^2. \tag{59}$$

Taking the time derivative of V yields

$$\begin{aligned}\dot{V} &= s\dot{s} \\ &= s\left(g - \hat{g} + (h\hat{h}^{-1} - 1)\hat{u}_2\right) - h\hat{h}^{-1}\left(k - \gamma\dot{\phi}\right)|s| \\ &= (g - \hat{g})s - h\hat{h}^{-1}\beta G|s| + (h\hat{h}^{-1} - 1)\hat{u}_2 s \\ &\quad - h\hat{h}^{-1}(\beta - 1)|\hat{u}_2||s| - h\hat{h}^{-1}\beta\eta|s| \\ &\quad + h\hat{h}^{-1}\gamma\dot{\phi}|s|, \end{aligned} \tag{60}$$

where γ is defined as

$$\gamma = \begin{cases} \beta^{-1}, & \text{if } \dot{\phi} \geq 0, \\ \beta, & \text{if } \dot{\phi} < 0. \end{cases} \tag{61}$$

From (27), (28), and (60), we can obtain the inequality such that

$$\dot{V} \leq \left(\dot{\phi} - \eta\right)|s|. \tag{62}$$

When $s > \phi$, we obtain the inequality from (59) and (62) such that

$$\frac{d}{dt}(s - \phi) \leq -\eta. \tag{63}$$

The inequality (63) means that the gap between s and ϕ always decreases. When $s < -\phi$, we also obtain the inequality from (59) and (62) such that

$$\frac{d}{dt}((-\phi) - s) \leq -\eta. \tag{64}$$

The inequality (64) also means that the gap between s and $-\phi$ always decreases. Therefore, after a sufficiently long time, $|s|$ surely becomes smaller than ϕ, i.e., the set $|s| \leq \phi$ is the invariant set.

The variable ϕ is the state of the system of (41). The equilibrium point of the system of (41) is $\frac{\beta(\hat{m}_2)k\left(v_1 - \dot{d}_r\right)}{\lambda}$, and the system of (41) is asymptotically stable. Thus, we can obtain the inequality such that

$$|s| \leq \frac{\beta(\hat{m}_2)k\left(v_1 - \dot{d}_r\right)}{\lambda}. \tag{65}$$

From (36), we obtain the dynamics for $\tilde{d}$ as follows:

$$\dot{\tilde{d}} = -\lambda\tilde{d} + s. \tag{66}$$

Because the system of (66) is asymptotically stable, $\tilde{d}$ converges to $\frac{s}{\lambda}$. Therefore, we can obtain the inequality such that

$$|\tilde{d}| \leq \frac{\beta(\hat{m}_2)k\left(v_1 - \dot{d}_r\right)}{\lambda^2}. \tag{67}$$

REFERENCES

[1] Ministry of Land, Infrastructure and Transport. (2018). *Road Statistics*. [Online]. Available: http://stat.molit.go.kr/portal/cate/engStatListPopup.do

[2] U. Bock and J. Y. Varchmin, "Enhancement of the occupancy of railroads using 'virtually coupled train formations,"' in *Proc. World Congr. Raillway Res. (WCRR)*, Tokyo, Japan, 1999, pp. 1–7.

[3] U. Bock and G. Bikker, "Design and development of a future freight train concept—'Virtually coupled train formations,"' *IFAC Proc. Volumes*, vol. 33, no. 9, pp. 395–400, Jun. 2000.

[4] S. Konig and E. Schnieder, "Modeling and simulation of an operation concept for future rail traffic," in *Proc. IEEE Intell. Transp. Syst. (ITSC)*, Aug. 2001, pp. 808–812.

[5] D.-I.-T. Ständer, D.-I.-J. Drewes, D.-W.-I.-I. Braun, and P. D.-I.-D. H. C. E. Schnieder, "Operational and safety concepts for railway operation with virtual train-sets," *IFAC Proc. Volumes*, vol. 39, no. 12, pp. 261–266, Jan. 2006.

[6] J. Goikoetxea, "Roadmap towards the wireless virtual coupling of trains," in *Proc. Int. Workshop Commun. Technol. Vehicles*, 2016, pp. 5–9.

[7] F. Flammini, S. Marrone, R. Nardone, A. Petrillo, S. Santini, and V. Vittorini, "Towards railway virtual coupling," in *Proc. IEEE Int. Conf. Elect. Syst. Aircr., Railway, Ship Propuls. Road Vehicles Int. Transp. Electrific. Conf. (ESARS-ITEC)*, Nov. 2018, pp. 1–6.

[8] C. Di Meo, M. Di Vaio, F. Flammini, R. Nardone, S. Santini, and V. Vittorini, "ERTMS/ETCS virtual coupling: Proof of concept and numerical analysis," *IEEE Trans. Intell. Transp. Syst.*, vol. 21, no. 6, pp. 2545–2556, Jun. 2020.

[9] T. Schumann, "Increase of capacity on the shinkansen high-speed line using virtual coupling," *Int. J. Transp. Develop. Integr.*, vol. 1, no. 4, pp. 666–676, 2017.

[10] H. Wilhelmi, T. Thieme, A. Henning, and C. Wagner, "Aerodynamic investigations of the effects of virtual coupling on two next generation trains," in *New Results in Numerical and Experimental Fluid Mechanics XI*. Cham, Switzerland: Springer, 2017, pp. 695–704.

[11] J. Winter, A. Lehner, and E. Polisky, "Electronic coupling of next generation trains," in *Proc. 3rd Int. Conf. Railway Technol., Res., Develop. Maintenance*, 2016, pp. 1–17.

[12] J. Felez, Y. Kim, and F. Borrelli, "A model predictive control approach for virtual coupling in railways," *IEEE Trans. Intell. Transp. Syst.*, vol. 20, no. 7, pp. 2728–2739, Jul. 2019.

[13] J. Slotine and W. Li, *Applied Nonlinear Control*. Upper Saddle River, NJ, USA: Prentice-Hall, 1991.

[14] S. E. Shladover, "PATH at 20—History and major milestones," *IEEE Trans. Intell. Transp. Syst.*, vol. 8, no. 4, pp. 584–592, Dec. 2007.

[15] K.-Y. Liang, J. Mårtensson, and K. H. Johansson, "Heavy-duty vehicle platoon formation for fuel efficiency," *IEEE Trans. Intell. Transp. Syst.*, vol. 17, no. 4, pp. 1051–1061, Apr. 2016.

[16] V. Turri, B. Besselink, and K. H. Johansson, "Cooperative look-ahead control for fuel-efficient and safe heavy-duty vehicle platooning," *IEEE Trans. Control Syst. Technol.*, vol. 25, no. 1, pp. 12–28, Jan. 2017.

[17] H. Dong, S. Gao, and B. Ning, "Cooperative control synthesis and stability analysis of multiple trains under moving signaling systems," *IEEE Trans. Intell. Transp. Syst.*, vol. 17, no. 10, pp. 2730–2738, Oct. 2016.

[18] S. Gao, H. Dong, B. Ning, and Q. Zhang, "Cooperative prescribed performance tracking control for multiple high-speed trains in moving block signaling system," *IEEE Trans. Intell. Transp. Syst.*, vol. 20, no. 7, pp. 2740–2749, Jul. 2019.

[19] S. Iwnicki, Ed., *Handbook of Railway Vehicle Dynamics*. Oxford, U.K.: Taylor & Francis, 2006.

[20] G. Goodwin, S. Graebe, and M. Salgado, *Control System Design*. Englewood Cliffs, NJ, USA: Prentice-Hall, 2001.

[21] R. Parise, H. Dittus, J. Winter, and A. Lehner, "Reasoning functional requirements for virtually coupled train sets: Communication," *IEEE Commun. Mag.*, vol. 57, no. 9, pp. 12–17, Sep. 2019.

Jaegeun Park (Graduate Student Member, IEEE) received the B.S. degree in electrical, electronics and communication engineering from the Korea University of Technology and Education, Cheonan, South Korea, in 2015, and the M.S. degree in information and communication engineering from the Daegu Gyeongbuk Institute of Science and Technology, Daegu, South Korea, in 2017, where he is currently pursuing the Ph.D. degree in information and communication engineering.

His current research interests include robust control of trains and resilient cyber-physical systems.

Byung-Hun Lee (Member, IEEE) received the B.S. degree in electronics engineering from Inha University, Incheon, South Korea, in 2011, and the M.S. and Ph.D. degrees in mechatronics from the Gwangju Institute of Science and Technology (GIST), Gwangju, South Korea, in 2013 and 2017, respectively.

He is currently a Senior Researcher with the Korea Railroad Research Institute (KRRI), Uiwang, South Korea. His current research interests include control theory and distributed control of multiagent systems.

Yongsoon Eun (Senior Member, IEEE) received the B.A. degree in mathematics and the B.S. and M.S.E. degrees in control and instrumentation engineering from Seoul National University, Seoul, South Korea, in 1922, 1994, and 1997, respectively, and the Ph.D. degree in electrical engineering and computer science from the University of Michigan, Ann Arbor, MI, USA, in 2003.

From 2003 to 2012, he was a Research Scientist with the Xerox Innovation Group, Webster, NY, USA, where he worked on technologies in the xerographic marking process and production inkjet printers. Since 2012, he has been with DGIST, Daegu, South Korea. He is currently a Professor with the Department of Information and Communication Engineering and the Director of the DGIST Resilient Cyber-Physical Systems Research Center. His current research interests include control systems with nonlinear sensors and actuators, control of quadrotors, communication network, industry 4.0 production systems, and resilient cyber-physical systems.